Thermal characterization of Bi_2Te_3/Sb_2Te_3 superlattices

M. N. Touzelbaev and P. Zhou
Department of Mechanical Engineering, Stanford University, Stanford, California 94305-3030

R. Venkatasubramanian
Center for Semiconductor Research, Research Triangle Institute, Research Triangle Park, Durham, North Carolina 27709-2195

K. E. Goodson[a)]
Department of Mechanical Engineering, Stanford University, Stanford, California 94305-3030

(Received 17 January 2000; accepted for publication 2 April 2001)

Superlattices offer the potential to enhance the figure of merit for thermoelectric cooling by increasing the Seebeck coefficient while decreasing the thermal conductivity compared to bulk samples. The large bulk value of *ZT* makes superlattices containing Bi_2Te_3 attractive for demonstrating benefits of using low-dimensional materials in thermoelectric applications. The present work describes measurements of the effective thermal conductivity normal to Bi_2Te_3/Sb_2Te_3 superlattices deposited on GaAs using noncontact pulsed laser heating and thermoreflectance thermometry. The data show a strong reduction in the effective thermal conductivity of the Bi_2Te_3/Sb_2Te_3 superlattices compared to bulk Bi_2Te_3, which can further increase thermoelectric figure of merit. The dependence of thermal conductivity on superlattice period is found to be weak, particularly at periods above 60 Å. This indicates that disorder in Bi_2Te_3/Sb_2Te_3 superlattices may limit the heat conduction process at shorter periods than in Si/Ge superlattices, for which measurements were previously reported in the literature. © *2001 American Institute of Physics*. [DOI: 10.1063/1.1374458]

I. INTRODUCTION

In the past few years, the application of superlattices to thermoelectric cooling has received considerable attention[1–4] due to its potential for increasing the associated figure of merit, $ZT=\sigma^2\epsilon T/\kappa$, where ϵ and κ are electrical and thermal conductivities, T is the temperature, and σ is the Seebeck coefficient. The large bulk value of the *ZT* made systems containing Bi_2Te_3 is a good choice for demonstrating the benefits of using low-dimensional materials in thermoelectric applications. Initial calculations predicting the *ZT* of superlattices containing Bi_2Te_3 showed[1] that carrier confinement effects can lead to an enhancement in the *ZT* of more than an order of magnitude over that of bulk samples. These predictions also showed that superlattices with smaller periods have a higher figure of merit. Further work[2,3] accounted for the tunneling of carriers between the well regions of the superlattice, which, as opposed to earlier predictions, reduces the *ZT* at small superlattice periods. The heat flow in the barrier regions of the superlattice was also predicted to decrease the *ZT*.[4]

Most of the previous research concentrated on the modification of charge transport parameters, while the phonon thermal conductivity was assumed not to vary with superlattice period. The phonon mean free path was estimated[1] to be of the order of 10 Å using the expression for thermal conductivity derived from kinetic theory. This low value of the mean free path suggests a small contribution of the well/barrier phonon boundary scattering to the total scattering rate at typical superlattice periods. These considerations led researchers to use the bulk thermal conductivity in their predictions for the thermoelectric figure of merit of superlattices.[1–4] The present study shows that the thermal conductivity of Bi_2Te_3/Sb_2Te_3 superlattices can be significantly lower than that of bulk samples making it a very important parameter in achieving a higher *ZT*.

Bi_2Te_3 is a highly anisotropic material due to the difference in strength between weak van der Waals bonds among the adjacent Te atoms and strong covalent bonds between Bi and Te atoms.[5] The thermal conductivity of bulk Bi_2Te_3 is 1.5 $W\,m^{-1}\,K^{-1}$ along the cleavage plane (perpendicular to the van der Waals bonding direction), while it reduces to values as low as 0.6 $W\,m^{-1}\,K^{-1}$ in the direction perpendicular to the cleavage plane.[6] The low thermal conductivity of Bi_2Te_3 is comparable to that of highly-disordered materials. In Bi_2Te_3, heat conduction proceeds through two types of carriers, phonons, and charge carriers. Goldsmid[7] has investigated mechanisms of heat conduction in Bi_2Te_3 and found that thermal conductivities of samples with higher doping concentrations were lower than those of samples with reduced doping levels. This effect is attributed to the transport of ionization energy by electron–hole pairs due to the changing carrier concentration in the direction of temperature gradient. It was also shown[7] that while the electronic contribution to thermal conductivity can be significant, lattice vibrations carry most of the thermal energy.

The thermal conductivity of bulk Bi_2Te_3 shows a temperature dependence typical of that of crystalline solids with a pronounced peak at cryogenic temperatures.[5] Scattering of

a)Electronic mail: goodson@vk.stanford.edu

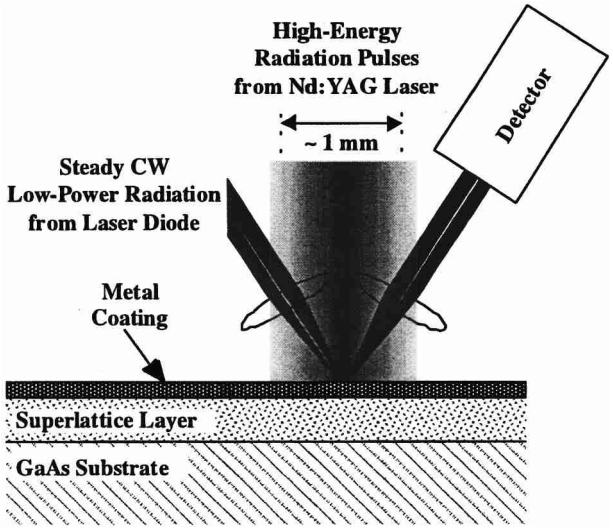

FIG. 1. The thermoreflectance method for measuring the vertical thermal resistance of Bi_2Te_3/Sb_2Te_3 superlattice layers.

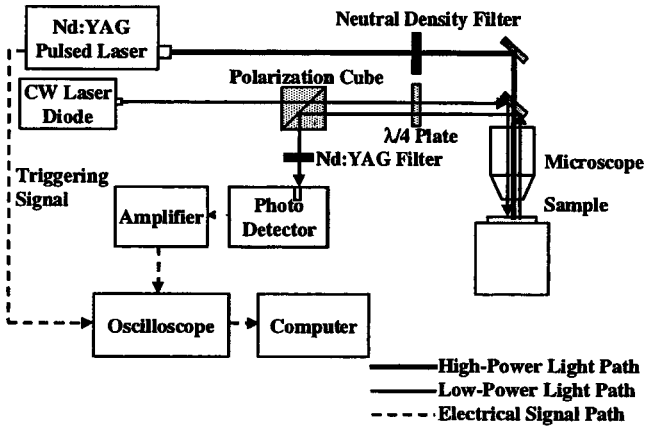

FIG. 2. Diagram describing the paths for radiation and electrical signals in the experimental setup.

phonons in Bi_2Te_3 at elevated temperatures mainly involves phonon–phonon processes, as evidenced by the $1/T$ dependence of the thermal conductivity with temperature.[8] The explanation for the reduction of the thermal conductivity with temperature within the framework of the Debye model is the increased scattering rate for phonons of higher frequencies which become increasingly populated as temperature increases. In this work, we present the results of thermal conductivity measurements and suggest that the data for small period superlattices can be explained by scattering at the interfaces between the constituent layers in a superlattice in addition to the intrinsic phonon–phonon scattering.

II. EXPERIMENTAL METHOD

Measurements of the effective thermal conductivity normal to Bi_2Te_3/Sb_2Te_3 superlattices with periods ranging from 40 to 120 Å deposited on GaAs are performed using noncontact pulsed laser heating and thermoreflectance thermometry.[9] The thermoreflectance technique, schematically depicted in Fig. 1, observes the temporal temperature decay using a probe laser after a brief heating of the metallized sample surface by the pump beam from a Nd:YAG laser. Figure 1 is only intended to demonstrate the principle of the measurement, while the details of the experimental setup are shown in Fig. 2. The probe beam coupled into a high-power optical microscope can be focused to the diffraction limit, while the pump beam has a diameter of around 1 mm at the sample surface to ensure one-dimensional heat conduction at measurement timescales. Band-pass filters block the radiation from the pump laser from leaking into the photodetector. The output of the high-bandwidth silicon photodetector is amplified and coupled into the 2 GHz bandwidth signal analyzer, from which the data are acquired and analyzed by a personal computer.

The laser heating and thermometry, used in this work, offers advantages over methods based on Joule heating and electrical-resistance thermometry in patterned bridges. Laser heating and thermometry can be used to map the variation of thermal properties in the plane of the layer. It also makes possible measurements on electrically conducting layers, such as films studied here, without the use of an insulating layer, which complicates data interpretation and increases the uncertainty for Joule-heating methods. Finally, the laser heating methods do not require patterning, which is an important benefit for alternative films whose chemical and mechanical stability may not be well understood for the purposes of fabrication and processing of microstructures.

The data analysis is performed by solving the heat diffusion equation in the frequency domain

$$\frac{i\cdot\omega}{\alpha_n}=\frac{d^2\theta_n}{dx_n^2}, \tag{1}$$

in a multilayer with boundary conditions given by

$$k_n\frac{d\theta_n(x_n=L_n)}{dx_n}=k_{n+1}\frac{d\theta_{n+1}(x_{n+1}=0)}{dx_{n+1}},$$
$$k_{n+1}\frac{d\theta_{n+1}(x_{n+1}=0)}{dx_{n+1}}=\frac{\theta_{n+1}(x_{n+1}=0)-\theta_n(x_n=L_n)}{R_n}, \tag{2}$$

where θ_n, k_n, and α_n are temperature, thermal conductivity, and diffusivity in nth layer and R_n is thermal resistance between the layers n and $n+1$. The output of the pump laser is sampled and transformed to the frequency domain to obtain the source term for the diffusion equation, which is then used to construct the solution in time domain. The solution of the equation and a least-squares algorithm for the fitting of the experimental data are directly integrated into the data acquisition software.

In contrast to some of the previous research,[9] the present measurements are performed on films with a much lower thermal conductivity. This relatively low thermal conductivity of the films in the present study aids with the measurement because of the long characteristic timescale of the temperature decay, which is on the order of several microseconds for films of thicknesses of around 1 μm. The longer timescale of the temperature decay also renders the details of the temporal shape of the pump beam unimportant due to the negligible thermal diffusion in the superlattice film during the heating pulse whose duration is around 8 ns.

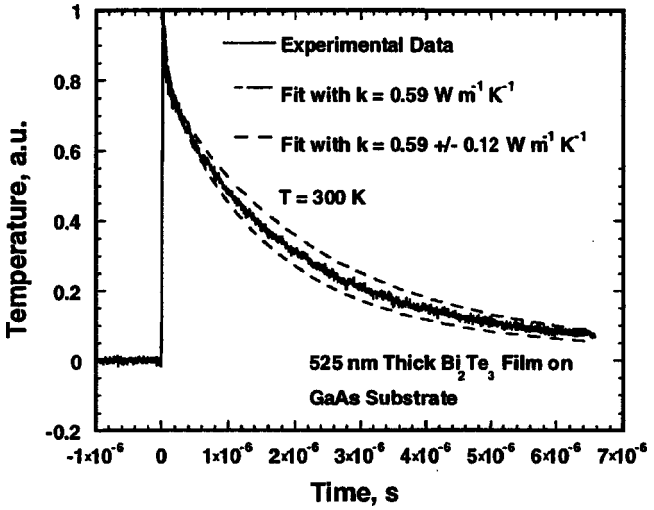

FIG. 3. The thermoreflectance signal and corresponding curvefit of the solution to the heat equation for the thermal conductivity measurement of Bi_2Te_3 thin film of a thickness of 525 nm deposited on GaAs.

Compared to mode-locked femtosecond lasers, also used for the thermoreflectance measurements,[10] a relatively long timescale of the pulse from Nd:YAG lasers is beneficial in avoiding initial transients governed by the conduction in the metal overlayer since the thermal diffusion length during the pulse is on the order of a micron for high-thermal conductivity metals such as gold or aluminum. Additionally, the low repetition rate of 10 Hz, compared to 76 MHz for modelocked lasers, ensures the complete dissipation of thermal energy between the pulses, which is important for the measurement of low thermal conductivity Bi_2Te_3/Sb_2Te_3 superlattices. A mismatch of three orders of magnitude between the thermal resistances of the metal layer and the superlattice for the layers of comparable thicknesses also reduces the measurement uncertainty since the only thermal property of the metal needed for the analysis is its thermal heat capacity.

Figure 3 shows the experimentally observed shape of the temperature decay fitted with the exact solution to the heat equation in the appropriate geometry. The measurement presented in Fig. 3 was performed on the 0.5 μm thick Bi_2Te_3 film and agrees with the published data[6] for bulk samples in the direction perpendicular to the cleavage plane, which is in the range between 0.6 to 0.77 $W\,m^{-1}\,K^{-1}$.

III. PHONON TRANSPORT MODELING

The reduction of the thermal conductivity of superlattices, coupled with the high mobility of charge carriers, may have a significant effect on the thermoelectric figure of merit. As discussed earlier, previous research used values of the bulk thermal conductivity in predicting figures of merit, but it is possible that optimization of the *ZT* may depend largely on the decreased thermal conductivity of superlattices. This effect gains more significance since the tunneling of charge carriers and lifting of valley degeneracy in a strained quantum well structure may reduce the benefits of the charge carrier confinement.[2,3] Therefore, it is important to understand the physical mechanisms of the thermal conductivity reduction in Bi_2Te_3/Sb_2Te_3 superlattices.

The mass fraction difference between the constituent layers in a superlattice structure leads to a formation of miniband gaps and augments the umklapp scattering by introducing additional reciprocal lattice vector.[11] However, this scattering mechanism alone cannot account for the observed strong reduction of the thermal conductivity of the superlattices compared to the bulk samples. The unexpectedly large reduction of the thermal conductivity can be explained by the longer than estimated value of 10 Å (Ref. 1) mean free path of main heat carriers. Recently, Chen[12] applied a semiclassical approach, based on particle transport formalism for phonons, to investigate superlattice thermal conductivity. In this work, we model thermal transport in superlattice structures using the Boltzmann transport equation with the analytical solutions obtained for the simplified boundary conditions between constituent materials.

The Peierls–Boltzmann transport equation in the relaxation time approximation is written as[13]

$$\vec{V}=\vec{\nabla}n+\frac{n}{\tau}=-\vec{V}\cdot\vec{\nabla}T\frac{\partial N_0}{\partial T}, \tag{3}$$

where n is the departure from the equilibrium state N_0, given by Bose–Einstein statistics, T is local temperature, V is phonon group velocity, and τ is the relaxation time. Assuming constant temperature gradient, a general solution of this equation is obtained as[13]

$$n=-\tau\vec{V}\cdot\vec{\nabla}T\frac{\partial N_0}{\partial T}\left[1+F(V,r_B)\exp\left(-\frac{|\vec{r}-\vec{r}_B|}{\tau V}\right)\right], \tag{4}$$

where $\vec{r}_B$ is the location of the boundary intercepted along direction θ as the particle is retraced back along its trajectory, and F is an arbitrary function not depending on the current coordinate z and can be suitably chosen to satisfy boundary conditions.

The mismatch of acoustic properties leads to the thermal boundary resistance even for perfect interfaces, which is especially evident for solid/liquid boundaries.[14] As opposed to that, the parameter governing transmission between two media, the acoustic impedance $Z=\rho V$, does not differ greatly for many solids. While for cryogenic temperatures, the acoustic mismatch theory correctly predicts the experimentally observed thermal boundary resistance between the solids, it fails to explain the data at temperatures above around 50 K.[14] The generally accepted explanation for this phenomenon is the effect of the imperfect interface, which becomes important as the dominant phonon wavelength approaches the scale of the interface roughness with increasing temperature. If any other boundary effects, such as dislocations and surface contaminants, are ignored, then we can introduce the transmission probability p to characterize phonon reflection and transmission near the interface, which for the case of superlattices, is similar to the specularity parameter for the solution in a single layer.[15]

For a single layer, a function F in Eq. (5) is readily obtained.[15] This result can also be extended to include the effects of additional boundaries apart from the immediately surrounding layer under consideration. Once function F describing departure from equilibrium in the near scattering boundaries is obtained, one can integrate over the contribu-

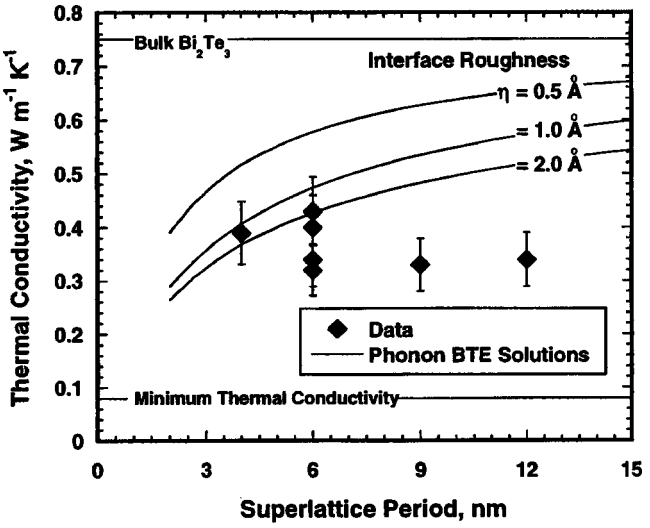

FIG. 4. Thermal conductivity of Bi_2Te_3/Sb_2Te_3 superlattices of a function of period.

tions to transport from all available modes at a given energy surface to obtain the next relation for the reduction of mean free in a direction perpendicular to the boundary:

$$R(z^*,\delta,p)=1+3\int_1^\infty F(\delta,p)\,\frac{\exp((z^*-\delta)t)-\exp(-\delta t)}{t^4}\,dt. \tag{5}$$

Counting the contribution of all phonon frequencies to heat transport, we can write for the thermal conductivity

$$k(z^*,p,L)=\frac{1}{3}\int_0^{\theta/T} C(x_\omega,T)V^2\tau(x_\omega,T) \times R\left[z^*,\frac{L}{V\tau(x_\omega,T)},p\right]d\omega, \tag{6}$$

where $x_\omega=\hbar\omega/(k_BT)$ is the dimensionless phonon frequency, $V=1500\,\mathrm{m\,s^{-1}}$ is the phonon velocity,[8] averaged over all polarization modes, and $\theta=142\,\mathrm{K}$ is the Debye temperature.[8] According to the Debye model for the density of states, the frequency dependent phonon specific heat is[13]

$$C(x_\omega,T)=9n_ak_B\left(\frac{T}{\theta}\right)^3\frac{x_\omega^4\exp(x_\omega)}{[\exp(x_\omega)-1]^2}. \tag{7}$$

The relaxation time for umklapp phonon scattering at high temperatures is modeled as[13]

$$\tau(\omega,T)=(B_UT^3x_\omega^2)^{-1}. \tag{8}$$

Parameter B_U is adjusted to give a value of $0.77\,\mathrm{W\,m^{-1}\,K^{-1}}$ for the bulk thermal conductivity of Bi_2Te_3. The functional dependence of phonon relaxation times at temperatures above the Debye temperature, established by Eq. (8), explains well the experimentally observed $1/T$ dependence of the Bi_2Te_3 thermal conductivity.[8]

IV. RESULTS AND DISCUSSION

The data presented in Fig. 4 show a strong reduction of the effective thermal conductivity of the Bi_2Te_3/Sb_2Te_3 superlattices compared to that of the bulk Bi_2Te_3. The thermal conductivity of the superlattices was measured to be as low as $0.3\,\mathrm{W\,m^{-1}\,K^{-1}}$ in the direction perpendicular to the cleavage plane. This is more than a factor of two reduction from the lowest reported bulk value of $0.6\,\mathrm{W\,m^{-1}\,K^{-1}}$. This is a remarkably low value considering the crystalline nature of this material. Figure 5 shows a transmission electron micrograph of the 60 Å/60 Å Bi_2Te_3/Sb_2Te_3 superlattice, grown under conditions[16,17] identical to the growth conditions of the samples under study. The image reveals that good quality interfaces were formed during the superlattice growth, especially if one considers the difficulty of sample preparation for ''soft'' materials, such as Bi_2Te_3.

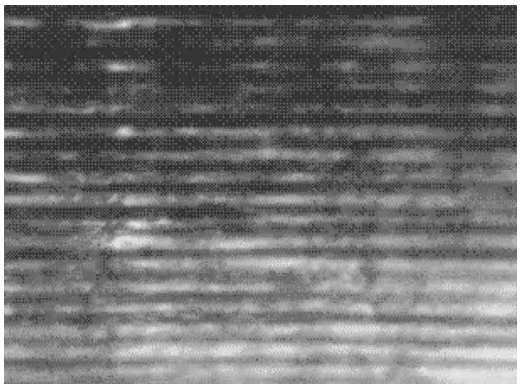

FIG. 5. Transmission electron micrograph of a 60 Å/60 Å Bi_2Te_3/Sb_2Te_3 superlattice.

Since the thermal conductivity of the bulk Bi_2Te_3 is low, it is also of interest to calculate a limit for its value. A study by Cahill *et al.*[18] showed that for some mixed crystalline solids, the thermal conductivity at room temperatures approaches values predicted using the Einstein limit for thermal conductivity, given as[18]

$$k_{\mathrm{train}}=\left(\frac{\pi}{6}\right)^{1/3}k_Bn^{2/3}\sum_i V_i\left(\frac{T}{\theta_i}\right)^2\int_0^{2\,\theta_i/T}\frac{x^3e^x}{(e^x-1)^2}\,dx, \tag{9}$$

where k_b is Boltzmann constant, n is the atomic number density, V is the phonon velocity, θ is Debye temperature, and the summation is over three polarization modes. In the present analysis, the phonon velocities and Debye temperatures for different polarization modes were replaced with the already averaged values, given in the Sec. III. The observed superlattice thermal conductivity is still significantly higher than the estimates based on Eq. (9).

Figure 4 shows predictions of the effective thermal conductivity normal to layers based on the model developed in the previous Sec. III, Eqs. (5) and (6). Also shown is the lower limit to the thermal conductivity calculated according to Eq. (9). The parameter p depends on the relative magnitude of the phonon wavelength compared to the mean roughness of the interface and can be related to the interface roughness and the wavelength of the incident wave as[13]

$$p(\lambda,\eta)=\exp\left[-\frac{16\pi^3\eta^2}{\lambda^2}\right], \tag{10}$$

where λ is the wavelength and η is the mean interface roughness.

As expected, calculations based on the semiclassical phonon transport theory predict increased thermal conductivity with the increased superlattice period, but the experimental data shows no such trend over the range of the studied periods. At small superlattice periods, data for the effective thermal conductivity of Bi_2Te_3/Sb_2Te_3 superlattices can be characterized by assuming an interface roughness on the order of an angstrom, while the agreement is poor for longer period superlattices. One explanation is a higher defect density at larger superlattice periods due to a higher mismatch stress between the constituent materials, leading to an additional phonon imperfection scattering near the boundaries. Previous research[19] measured the thermal conductivity of Si/Ge superlattices and found that for spatial periods greater than 130 Å, its value approaches that of highly-disordered solids. This effect was attributed to imperfections formed as the mechanical stresses exceed a critical value with the increasing spatial periods of superlattice. This research suggests that disorder in Bi_2Te_3/Sb_2Te_3 superlattices can limit heat conduction process at smaller superlattice periods.

In this work, we performed measurements of the effective thermal conductivity normal to the Bi_2Te_3/Sb_2Te_3 superlattices layers. Thermal conductivity of the superlattice layers was found to be significantly lower than the bulk value for Bi_2Te_3. We credit this unexpected reduction of the thermal conductivity to the relative importance of low frequency acoustic phonons with longer mean free paths. The mean free path of the heat-carrying phonons, estimated using Eqs. (6) and (8) without the boundary scattering term, is found to be on the order of 10 nm. This value of mean free path is an order of magnitude larger than previous estimates[1] based on the total heat capacity of Bi_2Te_3. As a result, we suggest that the scattering of heat-carrying phonons on well/barrier boundaries can reduce the thermal conductivity at superlattice periods of several nanometers by nearly a factor of two from the reported values for bulk Bi_2Te_3. At superlattice periods exceeding 60 Å, it is possible that the disorder due to increased mismatch stress further reduces thermal conductivity in addition to the boundary scattering. From this, we conclude that the thermoelectric figure of merit can be increased by as much as a factor of two due primarily to the decreased thermal conductivity in superlattices structures.

This work was performed with the support of DARPA and the Semiconductor Research Corporation through Contract No. SJ-461.

[1] L. D. Hicks and M. S. Dresselhaus, Phys. Rev. B **47**, 12727 (1993).
[2] J. O. Sofo and G. D. Mahan, Appl. Phys. Lett. **65**, 2690 (1994).
[3] D. A. Broido and T. L. Reinecke, Phys. Rev. B **51**, 13797 (1994).
[4] G. D. Mahan and H. B. Lyon, J. Appl. Phys. **76**, 1899 (1994).
[5] H. J. Goldsmid, *Thermoelectric Refrigeration* (Plenum, New York, 1964).
[6] Y. S. Touloukian, R. W. Powell, C. Y. Ho, and P. G. Klemens, *Thermophysical Properties of Matter* (Plenum, New York, 1970), Vol. 1.
[7] H. J. Goldsmid, Proc. Phys. Soc. **72**, 17 (1958).
[8] K. Yokota S. Katayama, J. J. Appl. Phys. **12**, 1205 (1973).
[9] K. E. Goodson, O. W. Kaeding, M. Roesler, and R. Zachai, J. Appl. Phys. **77**, 1385 (1995).
[10] W. S. Capinski and H. J. Maris, Rev. Sci. Instrum. **67**, 2720 (1996).
[11] S. Y. Ren and J. D. Dow, Phys. Rev. B **25**, 3750 (1982).
[12] G. Chen, Phys. Rev. B **57**, 14958 (1998).
[13] J. M. Ziman, *Electrons and Phonons* (Clarendon, Oxford, 1960).
[14] E. T. Swartz and R. O. Pohl, Rev. Mod. Phys. **61**, 605 (1989).
[15] E. H. Sondheimer, Adv. Phys. **1**, 1 (1952).
[16] R. Venkatasubramanian, T. Colpits, E. Watko, M. Lamvik, and N. El-Masry, J. Cryst. Growth **170**, 817 (1997).
[17] R. Venkatasubramanian, T. Colpits, E. Watko, and J. Hutchby, Proceddings of the 15th International Conference on Thermoelectrics (1996).
[18] D. G. Cahill, S. K. Watson, and R. O. Pohl, Phys. Rev. B **46**, 6131 (1992).
[19] S.-M. Lee, D. G. Cahill, and R. Venkatasubramanian, Appl. Phys. Lett. **70**, 2957 (1997).